PHYSICAL REVIEW C VOLUME 15, NUMBER 3 MARCH 1977

Nucleon-nucleon scattering analyses. II. Neutron-proton scattering from 0 to 425 MeV and proton-proton scattering from 1 to 500 MeV*

R. A. Arndt, R. H. Hackman, and L. D. Roper
Virginia Polytechnic Institute and State University, Blacksburg, Virginia 24061
(Received 23 June 1976)

The first paper of this series reported on energy-dependent and energy-independent phase-shift analyses of proton-proton elastic scattering data between 1 and 500 MeV. The present paper extends the analysis to include neutron-proton elastic scattering data between 0 and 425 MeV. Although this analysis is similar to those of the Livermore series, it differs in a number of important respects. First, a charge-splitting prescription has been employed for the isovector phases which includes Coulomb barrier effects and takes into account the difference in the masses between charged and uncharged pions. Second, a K-matrix formalism has been used to impose the constraints of the deuteron pole and the peripheral interaction (one-pion-exchange contribution) on the energy-dependent representation. Third, the neutron-proton and proton-proton scattering data have been fitted simultaneously in the search. The energy-dependent solution obtained uses 46 phenomenological parameters to represent 2670 data, with $\chi^2 = 2815$. A number of the neutron-proton phases have changed from the values obtained in Livermore X at higher energies, but the low-energy behavior is largely unaltered. A notable exception is the mixing parameter ϵ_1 which has been strongly affected by the deuteron pole. The proton-proton phases are changed very slightly from the paper I values as a result of the additional n-p constraints upon the $I = 1$ phases. We feel that the net result of these alterations is a more compact and reliable representation of nucleon-nucleon scattering in the energy range considered.

[NUCLEAR STRUCTURE Energy-dependent and energy-independent phase-shift combined analyses of 1–425 MeV n-p and 1–500 MeV p-p scattering data.]

I. INTRODUCTION

In this paper, we present the latest combined p-p and n-p scattering data analysis. The n-p data base[1-75] has grown sufficiently since the last energy-dependent analysis[76] to justify a reanalysis. In addition to the expanded data set there are two other important differences between this work and previous analyses. First, we have used the K-matrix formalism both for the calculation of the peripheral waves one-pion-exchange contribution (OPEC) and for the inclusion of the deuteron pole constraints. The mixing parameter ϵ_1, as determined in this manner, is considerably different than estimates obtained in previous analyses. Secondly, we have, for the first time, varied both the p-p and the n-p phases simultaneously.

This paper is the second of what is envisioned as a continuing series in anticipation of an influx of nucleon-nucleon scattering data from new high-intensity machines. In paper I of this series,[77] we published an analysis of the p-p scattering data between 1 and 500 MeV. The energy-dependent parametrization of the Livermore series was modified to account for low-energy Coulomb barrier effects and the $^1S_0$ scattering length and effective range were adjusted to obtain the best fit to the low-energy data.

In the present paper we have extended the analysis to include n-p scattering data between 1 and 425 MeV. This adjustment in the energy range for the n-p analysis is due primarily to the sparse and incomplete nature of the n-p data base above 425 MeV. The charge corrections of paper I for p-p scattering have been retained.

A complete discussion of our treatment of charge effects and of the energy-dependent representation is given in Secs. II and III. In keeping with our philosophy of providing a self-contained base upon which to build future analyses, we provide a complete listing of the n-p data used in this analysis in Sec. IV. In Sec. V we discuss the energy-dependent analysis and give the results of single-energy analyses at 25, 50, 100, 150, 200, 325, and 425 MeV.

II. CHARGE CORRECTIONS

In the present analysis, we differentiate between the p-p and n-p isovector phases according to the following recipe:

$$\delta_I^{pp} = \delta_I^{np}(m_\pi \to 135\ \text{MeV})\, C_I^2 ,$$

where δ^{pp} is the p-p isovector phase shift, δ^{np} is the n-p isovector phase shift, m_π is the pion mass (135 MeV for neutral pions and 136.5 MeV for n-p "averaged" pions), and C_I^2 is the "Coulomb

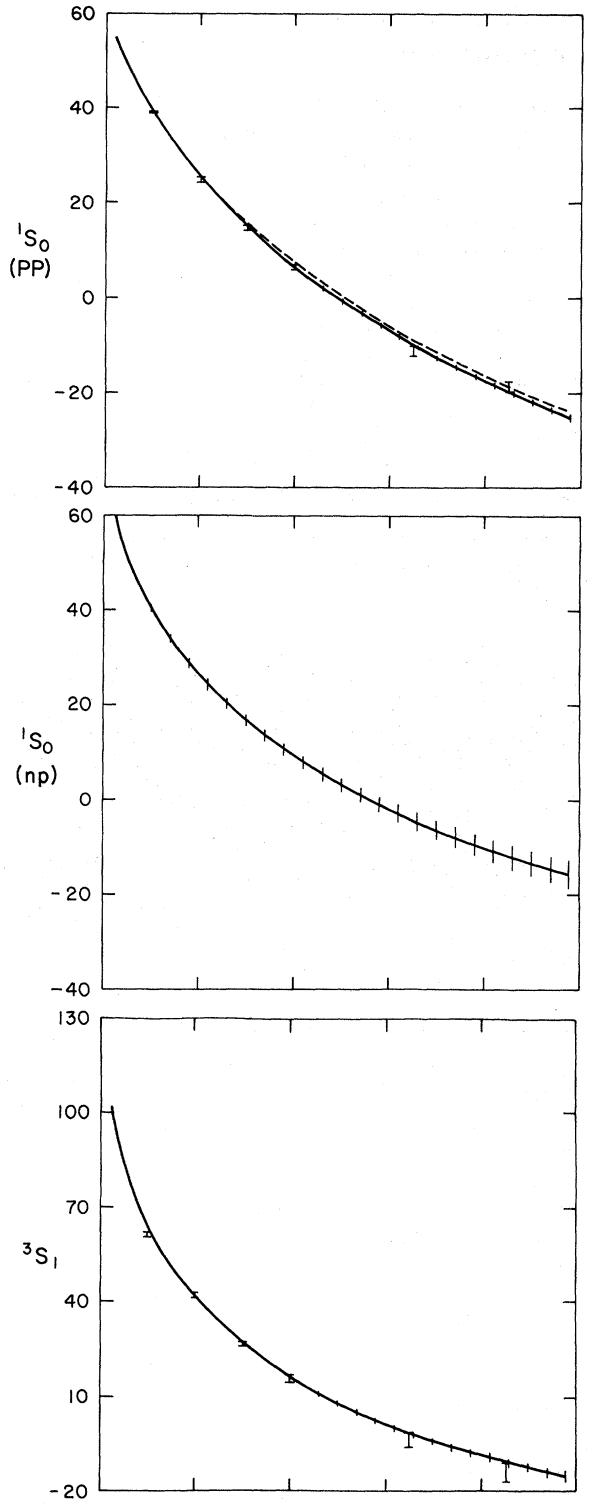

FIG. 1. Phase shifts from the energy-independent and energy-dependent solutions for the elastic n-p and p-p phases. The heavy solid lines refer to the OPEC contribution as calculated in the K-matrix formalism, the dotted lines refer to the p-p isovector phases, and the cross-hatched lines refer to the energy-dependent solution, the size of the cross-hatching indicating the size of the error bands. The error bands on the energy-dependent solution are defined in terms of a χ^2 change of 1.

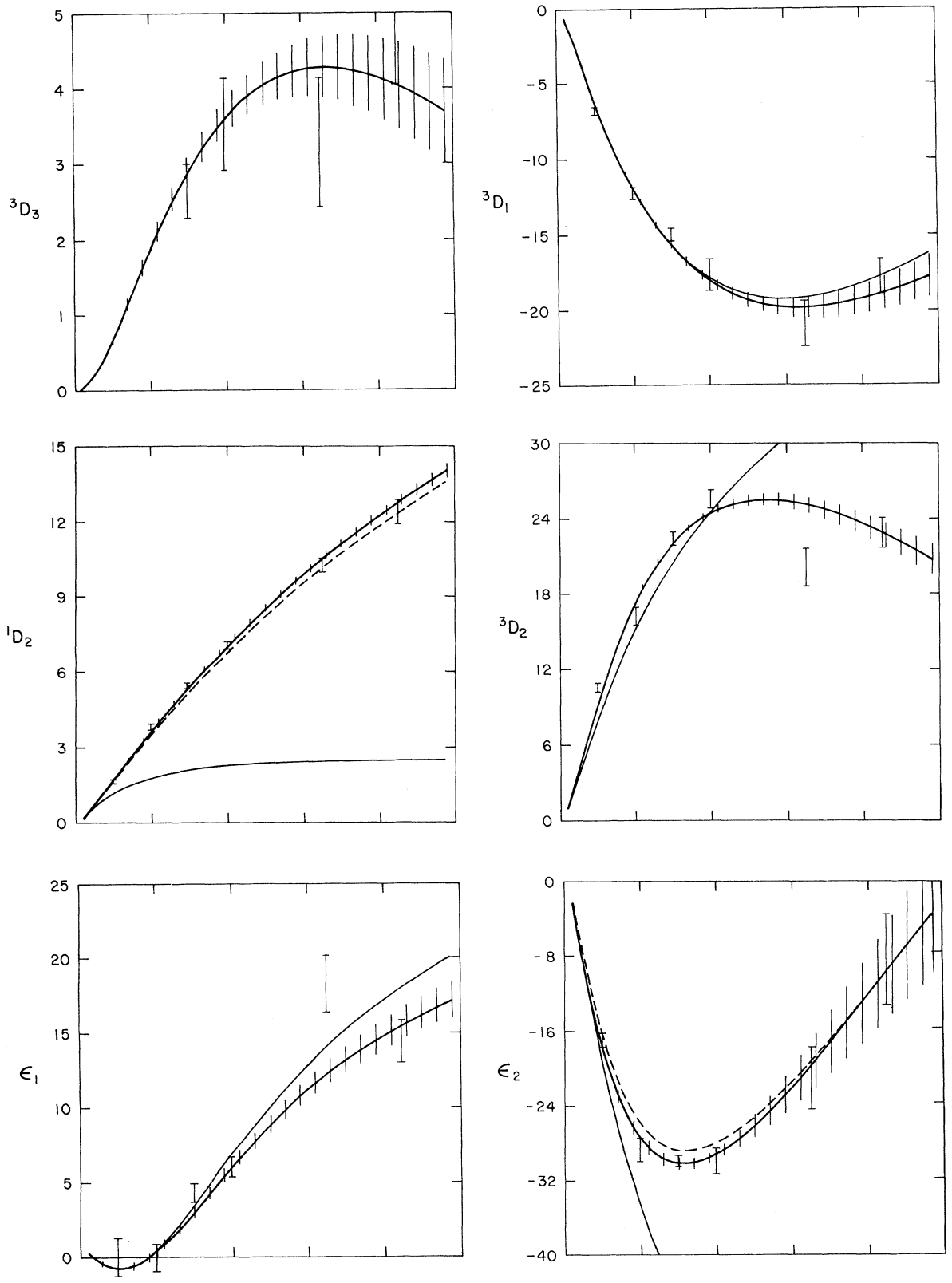

FIG. 1. (*Continued*)

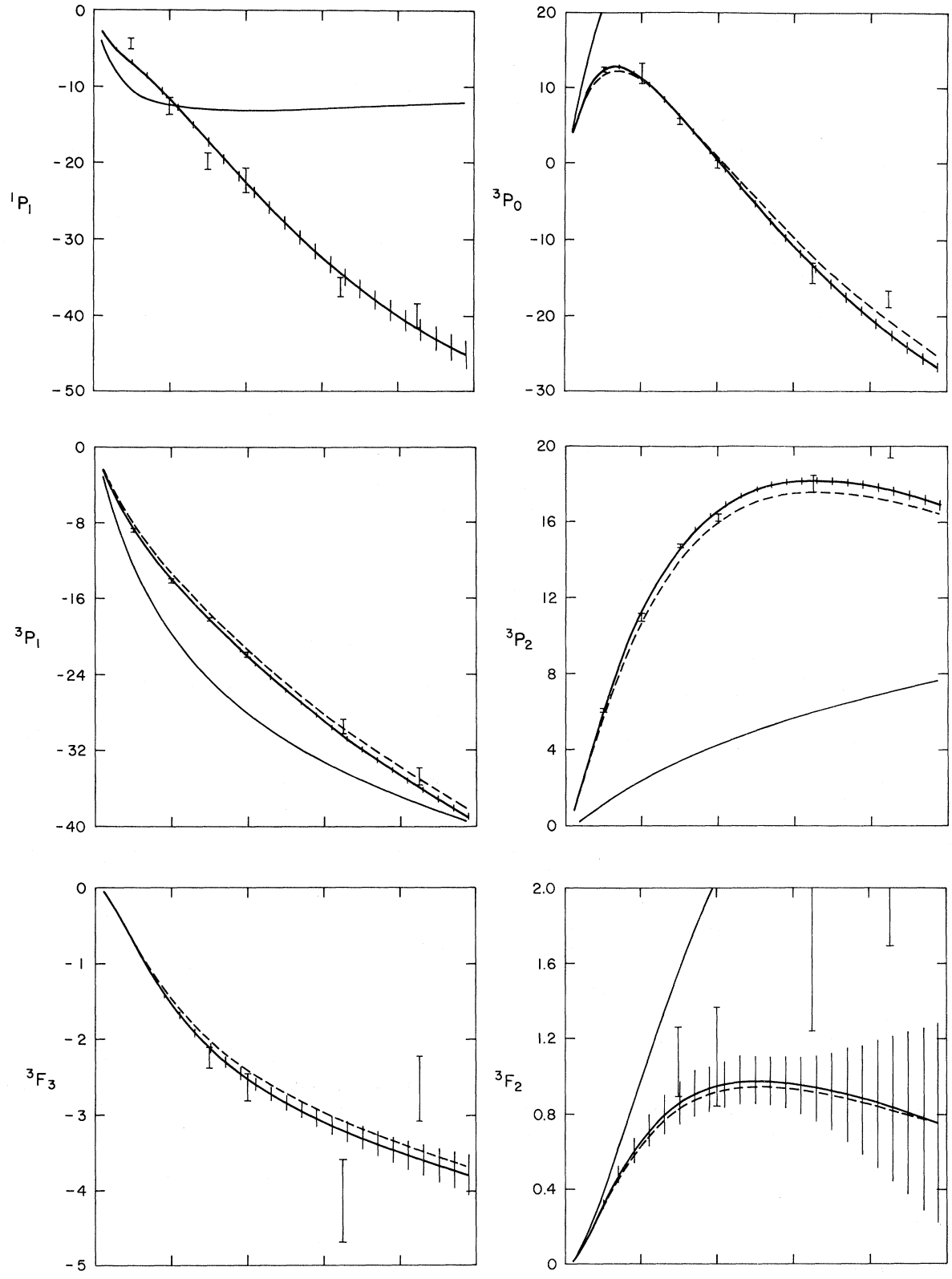

FIG. 1. (*Continued*)

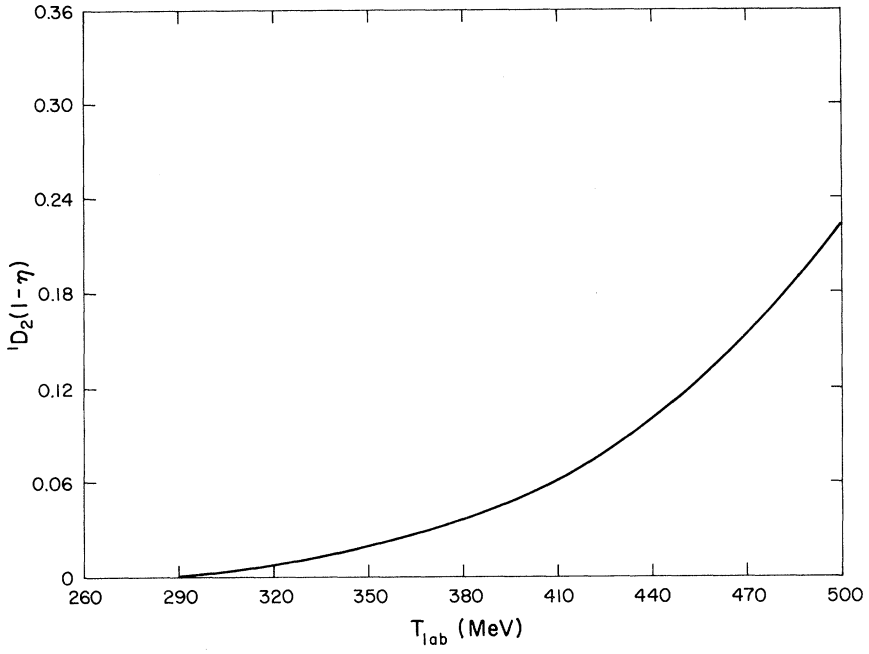

FIG. 2. The inelastic $^1D_2$ phase parameter from the energy-dependent solution.

barrier" factor defined by

$$C_l^2 = \frac{2\pi\eta}{e^{2\pi\eta}-1}\prod_{n=1}^{l}[1+(\eta/n)^2]$$

with $\eta = \alpha c/v_r$, v_r being the relative velocity and $\alpha = e^2/\hbar c$.

The change in the pion mass affects both the OPEC contribution and the phenomenological basis functions, which have left-hand cuts beginning at the two-pion exchange point and extending to negative infinity.

The effects of this "charge splitting" are depicted in Fig. 1. In all instances it is small, as compared to the errors on the results of the single-energy analyses.

This approximate "charge splitting" which we employ includes only those effects of which we are reasonably confident. The data itself is not discriminating enough to distinguish between δ^{pp} and δ^{np}, nor will it be for some time to come. In the course of the analysis, the isovector phases are essentially adjusted to fit the more abundant and precise p-p data.

III. ENERGY-DEPENDENT PARAMETRIZATION

The parametrization of the partial-wave amplitudes involving the deuteron state ($I=0$, $J=1$) is quite involved and we present a complete discussion of our methods in Appendix A. For all other partial-wave phase shifts, we use the basic form

$$\delta_l = \delta_l^{\mathrm{OPEC}} + \sum_i \alpha_{li} f_{li},$$

where the f_{li} are the phenomenological energy-dependent expansion bases,[76] α_{li} are the parameters to be adjusted in the course of the analysis, and δ_l^{OPEC} represents certain "theoretical constraints" imposed on the solution. This form differs from those used in previous analyses[76] primarily in the nature of the "theoretical constraints" and their method of imposition, which we discuss below.

For the uncoupled singlet S-wave states (δ_0^{np} and δ_0^{pp}) we have continued to use the modified effective-range expansions for δ_0^{OPEC} as described in Refs. 76 and 77. In all remaining partial waves, δ_l^{OPEC} represents the one-pion-exchange contribution.

The OPEC values for the remaining partial waves are calculated by identifying the Born approximation to this contribution B_l^{π} with the elements of a partial-wave K matrix defined by

$$S = (1+iK)(1-iK)^{-1}. \tag{1}$$

For uncoupled states this leads to

$$\tan\delta_l = B_l^{\pi},$$

while for coupled states the expression

$$K = \begin{pmatrix} B_- & B_0 \\ B_0 & B_+ \end{pmatrix},$$

TABLE I. n-p data from 0.493 to 425.0 MeV.

Energy (MeV)	No. and type of data	Angular range (c.m.) (deg)	% data std. error	% norm. std. error	M value	Predicted norm.	References	Comments
0.493	$1\sigma_T$		0.002	0.000	1.61	1.000	1	a
0.841	$1\sigma_T$		0.003	0.000	2.56	1.000	2	b
1.005	$1\sigma_T$		0.004	0.000	0.94	1.000	3	a
1.161	$1\sigma_T$		0.003	0.000	2.87	1.000	2	b
1.312	$1\sigma_T$		0.005	0.000	0.03	1.000	4	a
1.453	$1\sigma_T$		0.003	0.000	1.42	1.000	2	b
1.750	$1\sigma_T$		0.004	0.000	1.86	1.000	2	b
2.045	$1\sigma_T$		0.004	0.000	2.06	1.000	2	b
2.346	$1\sigma_T$		0.005	0.000	2.16	1.000	2	b
2.530	$1\sigma_T$		0.004	0.000	2.88	1.000	3	a
2.719	$1\sigma_T$		0.005	0.000	0.22	1.000	2	b
3.186	$1\sigma_T$		0.003	0.000	0.02	1.000	1	a
3.324	$1\sigma_T$		0.005	0.000	1.84	1.000	2	b
4.375	$1\sigma_T$		0.005	0.000	0.06	1.000	2	b
4.748	$1\sigma_T$		0.004	0.000	0.55	1.000	5	a
5.858	$1\sigma_T$		0.006	0.000	0.03	1.000	2	b
7.170	$1\sigma_T$		0.016	0.000	0.12	1.000	6	c
7.849	$1\sigma_T$		0.006	0.000	0.60	1.000	2	b
8.770	$1\sigma_T$		0.009	0.000	3.17	1.000	6	c
9.885	$1\sigma_T$		0.008	0.000	7.62	1.000	2	b
10.420	$1\sigma_T$		0.022	0.000	2.02	1.000	6	c
11.000	$1P$	90–90	0.005	0.000	0.00	1.000	7	b
11.130	$1\sigma_T$		0.023	0.000	1.06	1.000	6	c
11.918	$1\sigma_T$		0.013	0.000	0.56	1.000	2	b
13.130	$1\sigma_T$		0.027	0.000	1.24	1.000	6	c
13.924	$1\sigma_T$		0.017	0.000	0.21	1.000	2	b
14.000	3σ	80–100	0.022	0.016	0.27	1.008	8	b,d
14.020	$1\sigma_T$		0.014	0.000	7.29	1.000	6	c
14.100	8σ	48–154	0.039	9.000	0.19	1.055	9	c
14.100	16σ	11–92	0.075	9.000	0.20	1.004	10	c
14.100	6σ	70–173	0.037	0.040	0.17	1.031	11	c
14.100	$1\sigma_T$		0.007	0.000	0.00	1.000	12	c
15.700	16σ	56–161	0.001	9.000	0.70	8.811	13	c
15.800	$1\sigma_T$		0.049	0.020	6.01	1.019	14	c
15.963	$1\sigma_T$		0.022	0.000	0.25	1.000	2	b
16.200	$3P$	70–130	0.009	0.000	0.19	1.000	15	b
16.400	$1\sigma_T$		0.029	0.000	0.13	1.000	14	c
16.400	$3P$	100–140	0.024	0.093	0.68	0.997	16	c
16.400	$4P$	90–150	0.009	0.000	0.23	1.000	17	b
16.800	$1P$	90–90	0.006	0.000	0.00	1.000	7	b
16.900	$4P$	40–140	0.005	0.060	1.51	0.997	18	b
17.800	$1\sigma_T$		0.016	0.000	2.22	1.000	19	c
17.920	$1\sigma_T$		0.028	0.000	1.59	1.000	2	b
18.400	$1\sigma_T$		0.027	0.000	0.35	1.000	14	c
19.600	$1\sigma_T$		0.005	0.000	0.27	1.000	20	c
19.600	$1\sigma_T$		0.006	0.000	0.47	1.000	21	c
19.600	$1\sigma_T$		0.053	0.020	0.97	0.993	14	c
19.957	$1\sigma_T$		0.035	0.000	1.26	1.000	2	b
20.500	$1\sigma_T$		0.023	0.000	0.61	1.000	14	c
20.500	$9P$	21–100	0.054	0.188	0.84	0.882	22	c
20.600	$1\sigma_T$		0.021	0.000	0.01	1.000	19	c
21.100	$6P$	40–140	0.006	0.030	3.42	1.010	18	b
21.600	$7P$	50–170	0.005	1.000	1.14	0.789	17	b,e
21.900	$1\sigma_T$		0.046	0.020	0.79	1.007	14	c
22.500	$1\sigma_T$		0.047	0.020	0.91	1.008	14	c
22.500	12σ	65–175	0.053	9.000	0.45	1.017	23	c
22.500	6σ	7–51	0.059	0.033	0.53	1.004	24	c
23.100	$4C_{NN}$	130–174	0.026	0.000	2.51	1.000	25	c

TABLE I. (*Continued*)

Energy (MeV)	No. and type of data	Angular range (c.m.) (deg)	% data std. error	% norm. std. error	M value	Predicted norm.	References	Comments
23.100	$6P$	50–150	0.009	0.040	1.04	1.002	26	c
23.100	$2P$	140–150	0.007	0.200	1.51	1.306	7	b
23.700	$1\sigma_T$		0.020	0.000	0.08	1.000	14	c
23.700	$4P$	80–140	0.022	0.109	0.48	1.057	16	c
23.700	$1\sigma_T$		0.004	0.000	0.29	1.000	20	c
24.000	4σ	89–164	0.015	0.005	1.28	1.006	27	a
24.000	4σ	71–157	0.028	9.000	0.19	1.000	28	b
24.000	2σ	39–50	0.018	0.000	0.14	1.000	29	b,f
24.630	$1\sigma_T$		0.006	0.030	0.00	1.002	30	b
25.300	$1\sigma_T$		0.024	0.000	2.11	1.000	14	c
25.300	$1\sigma_T$		0.036	0.020	0.61	1.008	19	d
25.800	8σ	20–90	0.029	0.030	0.61	1.020	31	b,g
25.800	8σ	89–178	0.025	0.030	0.53	0.995	31	b,g
25.900	$1\sigma_T$		0.035	0.020	0.71	0.992	14	c
27.200	5σ	71–157	0.031	9.000	0.24	0.994	28	b
27.500	8σ	7–72	0.067	0.030	0.11	0.986	24	c
27.500	3σ	159–173	0.055	9.000	0.78	1.135	24	c
28.000	$1\sigma_T$		0.006	0.000	2.40	1.000	20	c
28.000	$1\sigma_T$		0.033	0.020	1.00	1.010	14	c
28.300	$1\sigma_T$		0.030	0.000	0.94	1.000	19	c
29.000	$1\sigma_T$		0.033	0.020	0.91	1.010	19	c
29.250	$1\sigma_T$		0.008	0.030	0.05	1.006	30	b
29.600	$1\sigma_T$		0.030	0.020	0.16	1.004	14	c
29.600	$3P$	60–120	0.014	0.100	0.21	0.959	7	b
29.600	$11P$	50–150	0.017	0.125	0.21	1.000	32	b
30.000	$9P$	21–100	0.031	0.083	1.20	1.031	22	c
30.000	$3P$	139–158	0.016	0.083	1.26	1.031	22	c
32.500	$1\sigma_T$		0.026	0.020	0.10	0.996	14	c
32.500	9σ	7–82	0.074	0.021	1.24	0.963	24	c
32.500	6σ	129–173	0.050	0.040	1.15	1.509	24	c
33.100	$1\sigma_T$		0.025	0.020	0.01	0.999	14	c
34.000	$1\sigma_T$		0.027	0.020	0.54	1.009	14	c
36.340	$1\sigma_T$		0.008	0.030	0.02	0.995	30	b
37.500	10σ	7–92	0.072	0.020	0.48	0.989	24	c
37.500	7σ	118–173	0.052	0.040	1.04	1.077	24	c
38.000	$1\sigma_T$		0.034	0.026	1.08	1.017	33	c
38.500	$1\sigma_T$		0.026	0.020	0.69	1.010	14	c
39.560	$1\sigma_T$		0.008	0.030	0.04	0.994	30	b
40.000	$1\sigma_T$		0.026	0.020	0.05	1.003	14	c
40.000	$9P$	21–101	0.035	0.106	0.86	0.942	22	c
40.000	$6P$	109–158	0.015	0.106	0.68	0.945	22	c
41.100	$1\sigma_T$		0.025	0.020	1.23	1.014	14	c
42.500	11σ	7–102	0.074	0.020	1.04	0.992	24	c
42.500	11σ	78–173	0.062	0.040	1.42	1.060	24	c
42.500	$1\sigma_T$		0.026	0.020	1.35	1.015	14	c
44.000	$1\sigma_T$		0.025	0.020	0.94	1.012	14	c
45.500	$1\sigma_T$		0.085	0.022	0.14	0.998	37	c
45.500	$1\sigma_T$		0.025	0.020	0.00	1.000	14	c
46.180	$1\sigma_T$		0.009	0.030	0.07	0.992	30	b
47.500	11σ	7–102	0.067	0.020	1.30	0.985	24	c
47.500	11σ	78–173	0.063	0.040	1.42	1.041	24	c
48.800	$1\sigma_T$		0.024	0.020	0.85	1.012	14	c
49.060	$1\sigma_T$		0.009	0.030	0.27	1.015	30	b
50.000	$9P$	21–101	0.026	0.047	0.24	0.972	22	c
50.000	$6P$	99–158	0.015	0.047	0.82	0.993	22	c
50.000	8σ	20–90	0.029	0.030	0.63	1.004	34	b,g
50.000	12σ	69–173	0.020	0.030	0.69	1.001	34	b,g
52.500	12σ	7–112	0.071	0.017	1.18	0.981	24	c

TABLE I. (*Continued*)

Energy (MeV)	No. and type of data	Angular range (c.m.) (deg)	% data std. error	% norm. std. error	M value	Predicted norm.	References	Comments
52.500	11σ	78–173	0.072	0.038	0.92	1.009	24	c
52.500	$1\sigma_T$		0.023	0.020	1.01	1.013	14	c
54.370	$1\sigma_T$		0.008	0.030	0.09	0.991	30	b
56.600	$1\sigma_T$		0.022	0.020	0.09	1.004	14	c
57.500	12σ	7–112	0.072	0.020	0.74	0.981	24	c
57.500	11σ	78–173	0.076	0.040	1.63	1.032	24	c
58.800	$1\sigma_T$		0.021	0.020	0.01	1.001	14	c
58.800	9σ	11–42	0.053	0.080	0.95	1.065	35	b
59.350	$1\sigma_T$		0.016	0.030	0.07	1.007	30	b
60.000	$9P$	21–101	0.022	0.039	1.37	1.090	22	c
60.000	$7P$	99–158	0.012	0.039	1.83	1.026	22	c
60.900	9σ	90–170	0.027	9.000	1.21	1.118	36	b,h
62.500	12σ	7–112	0.071	0.020	1.61	1.007	24	c
62.500	11σ	78–173	0.078	0.040	1.58	1.074	24	c
63.000	$1\sigma_T$		0.024	0.016	0.09	0.997	33	c
66.100	$1\sigma_T$		0.021	0.020	0.67	1.011	14	c
67.500	9σ	11–42	0.054	0.050	1.53	1.069	35	b
68.900	$1\sigma_T$		0.021	0.020	0.48	1.010	14	c
70.000	12σ	7–122	0.062	0.020	1.57	1.003	24	c
70.000	11σ	78–173	0.065	0.040	1.43	1.098	24	c
70.000	$9P$	21–101	0.026	0.039	2.00	1.119	22	c
70.000	$7P$	98–158	0.026	0.039	0.86	1.022	22	c
72.000	$1\sigma_T$		0.022	0.020	3.51	1.026	14	c
75.300	$1\sigma_T$		0.036	0.020	0.00	1.000	14	c
76.700	11σ	11–49	0.050	0.050	2.66	1.148	35	b
80.000	12σ	7–112	0.067	0.020	2.15	1.026	24	c
80.000	11σ	78–173	0.080	0.040	0.95	1.038	24	c
80.000	$9P$	21–101	0.032	0.042	0.80	1.075	22	c
80.000	$7P$	98–158	0.016	0.042	0.50	0.978	22	c
82.800	$1\sigma_T$		0.021	0.020	2.67	1.023	14	c
86.500	11σ	11–49	0.052	0.050	2.47	1.172	35	b
86.900	$1\sigma_T$		0.022	0.020	1.00	1.013	14	c
88.000	$1\sigma_T$		0.024	0.023	0.87	0.985	37	c
88.000	$1\sigma_T$		0.024	0.023	0.04	0.997	37	c
88.000	$1\sigma_T$		0.020	0.000	2.13	1.000	38	c
89.500	13σ	7–122	0.071	0.020	1.52	1.030	24	c
89.500	11σ	78–173	0.090	0.040	0.94	1.037	24	c
90.000	$9P$	21–101	0.052	0.051	0.79	1.074	22	c
90.000	$7P$	98–158	0.022	0.051	0.34	0.983	22	c
91.000	25σ	59–176	0.034	9.000	0.92	1.019	39	c
91.000	$1\sigma_T$		0.021	0.020	0.94	1.014	14	c
95.000	$1\sigma_T$		0.039	0.020	0.54	1.007	33	c
95.000	$15P$	22–159	0.042	0.080	2.15	1.081	40	c
96.800	11σ	11–49	0.057	0.050	1.88	1.096	35	b
99.000	$1\sigma_T$		0.021	0.000	3.59	1.000	38	c
99.000	13σ	7–122	0.078	0.017	1.57	1.022	24	c
99.000	11σ	78–173	0.105	0.038	1.26	0.972	24	c
100.000	$9P$	21–101	0.083	0.073	0.38	0.987	22	c
100.000	$7P$	98–158	0.036	0.073	0.76	0.969	22	c
100.000	$1\sigma_T$		0.024	0.020	0.00	1.000	14	c
105.000	7σ	6–61	0.087	0.080	0.39	0.924	41	c
105.000	$1\sigma_T$		0.023	0.020	0.52	0.991	14	c
107.600	11σ	12–50	0.061	0.050	1.70	1.071	35	b
108.500	13σ	7–122	0.093	0.020	1.65	1.014	24	c
108.500	11σ	78–173	0.123	0.040	1.97	0.973	24	c
110.000	$9P$	22–102	0.116	0.100	1.17	0.985	22	c
110.000	$7P$	98–158	0.048	0.100	1.45	0.944	22	c
110.000	$1\sigma_T$		0.021	0.000	4.50	1.000	38	c

TABLE I. (*Continued*)

Energy (MeV)	No. and type of data	Angular range (c.m.) (deg)	% data std. error	% norm. std. error	M value	Predicted norm.	References	Comments
110.000	$1\sigma_T$		0.032	0.020	2.71	0.983	14	c
118.800	11σ	12–50	0.069	0.050	1.55	1.067	35	b
120.000	$1\sigma_T$		0.022	0.000	3.94	1.000	38	c
120.000	$9P$	22–102	0.171	0.149	0.52	0.996	22	c
120.000	$7P$	98–158	0.080	0.149	0.78	0.952	22	c
126.000	$6P$	33–81	0.048	0.100	0.45	0.948	42	c
126.000	$1\sigma_T$		0.035	0.016	0.01	1.001	33	c
128.000	10σ	78–169	0.037	0.022	0.64	0.983	43	c
128.000	$10P$	78–169	0.023	0.100	1.79	0.958	43	c
128.000	$5D_T$	124–160	0.146	0.000	1.54	1.000	44	c
128.000	$1D_T$	170–170	0.209	0.000	0.01	1.000	45	c
128.500	$3A_T$,	139–163	0.376	0.000	1.61	1.000	46	c
129.000	15σ	73–176	0.049	0.065	0.69	0.999	47	c
129.400	$1\sigma_T$		0.021	0.000	3.16	1.000	38	c
130.000	14σ	25–155	0.107	0.032	0.87	1.038	48	c
130.500	11σ	11–50	0.058	0.050	1.65	1.042	35	b
135.000	$5A$	42–83	0.127	0.040	0.78	1.001	49	c
135.000	9σ	32–92	0.196	0.160	0.52	0.921	50	b,g
135.000	16σ	76–167	0.031	0.070	1.00	0.937	50	b,g
137.000	7σ	6–61	0.094	0.050	0.50	1.041	41	c
137.000	$5R$	43–83	0.124	0.000	0.76	1.000	49	c
140.000	$1\sigma_T$		0.107	0.000	0.44	1.000	51	c
140.000	$14P$	20–159	0.022	0.070	1.58	0.938	52	c
140.900	$1\sigma_T$		0.021	0.000	5.46	1.000	38	c
143.800	11σ	11–50	0.059	0.050	0.36	1.023	35	b
143.000	$8P$	41–118	0.022	1.000	1.10	1.141	53	c
150.000	16σ	63–176	0.038	0.065	0.97	0.985	47	c
150.900	$1\sigma_T$		0.020	0.000	6.23	1.000	38	c
152.000	13σ	77–169	0.021	1.000	2.22	0.899	54	b,i
153.000	$1\sigma_T$		0.025	0.020	2.21	1.019	33	c
155.400	11σ	11–50	0.048	0.050	2.83	1.052	35	b
156.000	$1\sigma_T$		0.173	0.000	0.09	1.000	51	c
168.500	11σ	11–50	0.052	0.050	1.66	1.051	35	b
181.800	11σ	11–50	0.058	0.050	1.05	1.070	35	b
195.600	11σ	11–50	0.068	0.050	1.63	1.017	35	b
197.000	$3D_T$	126–147	0.082	0.000	0.40	1.000	55	c
199.000	8σ	76–158	0.024	9.000	0.60	0.967	56	c
199.000	$8P$	76–158	0.015	0.100	1.03	0.974	56	c
200.000	20σ	6–173	0.111	0.020	1.54	0.968	56	c
200.000	$1\sigma_T$		0.022	0.000	1.52	1.000	56	c
203.000	$5R_T$	139–179	0.086	0.140	0.65	1.069	58	c
210.000	11σ	11–51	0.080	0.050	1.22	0.999	35	b
212.000	$5D$	40–80	0.224	0.000	0.76	1.000	59	c
217.000	$6P$	40–90	0.037	0.120	0.55	1.032	60	c
224.300	11σ	11–51	0.088	0.050	0.84	0.967	35	b
239.500	11σ	11–51	0.100	0.050	0.55	1.059	35	b
260.000	15σ	37–180	0.171	0.040	1.92	1.022	61	c
267.200	11σ	11–51	0.083	0.050	1.22	0.973	35	b
270.000	$1\sigma_T$		0.040	0.000	0.18	1.000	62	c
290.000	3σ	10–37	0.204	0.100	0.05	0.992	63	c
300.000	15σ	35–175	0.094	0.100	1.32	1.048	64	c
309.600	11σ	11–52	0.138	0.050	1.30	0.963	35	b
310.000	$19P$	21–164	0.053	0.040	1.15	0.996	65	c
310.000	$8P$	33–141	0.025	0.030	2.91	1.007	66	c
343.800	11σ	11–52	0.174	0.050	1.12	1.037	35	b
350.000	$1\sigma_T$		0.019	0.000	1.02	1.000	67	c
350.000	17σ	114–173	0.013	0.030	0.55	0.983	68	c

TABLE I. (*Continued*)

Energy (MeV)	No. and type of data	Angular range (c.m.) (deg)	% data std. error	% norm. std. error	M value	Predicted norm.	References	Comments
350.000	$10P$	46–158	0.027	9.000	2.02	1.005	69	a, c
380.000	$1\sigma_T$		0.055	0.000	1.38	1.000	70	c
380.000	14σ	36–180	0.137	0.180	1.78	1.092	71	c
390.200	11σ	11–53	0.178	0.050	1.09	0.988	35	b
400.000	21σ	12–180	0.095	0.030	1.72	1.053	72	c
400.000	$8P$	33–144	0.042	0.030	3.46	0.966	65	c
410.000	$1\sigma_T$		0.036	0.000	4.78	1.000	73	c
421.000	42σ	151–179	0.065	9.000	1.39	0.803	75	b, j
425.000	$3P$	43–90	0.013	0.047	6.18	0.980	74	a
425.000	$3D$	43–90	0.061	0.000	0.72	1.000	74	a
425.000	$3R$	43–90	0.042	0.000	2.20	1.000	74	a
425.000	$3A$	43–90	0.053	0.000	4.33	1.000	74	a

[a] Comments pertinent to this data set were given by M. H. McGregor, R. A. Arndt, and R. M. Wright, Phys. Rev. 182, 1714 (1969).

[b] New data which were not included in the analyses referenced in comments (a) and (c).

[c] Comments pertinent to this data set were given by M. H. McGregor, R. A. Arndt, and R. M. Wright, Phys. Rev. 173, 1272 (1968).

[d] These data were listed in Ref. 8 as anisotropy measurements. There are no provisions for such measurements in our analysis code. To utilize these measurements in our analysis, we have taken

$$\frac{d\sigma(\theta)}{d\Omega} = \left(\frac{1}{R(\theta)}\right)\frac{d\sigma(180°)}{d\Omega} \pm \frac{d\sigma(180°)}{d\Omega}\,\Delta\left(\frac{1}{R(\theta)}\right)$$

with a normalization uncertainty of

$$\Delta\left(\frac{d\sigma(180°)}{d\Omega}\right)\Big/\frac{d\sigma(180°)}{d\Omega}\,,$$

where

$$\Delta\left(\frac{d\sigma(180°)}{d\Omega}\right) \text{ and } \frac{d\sigma(180°)}{d\Omega}$$

were derived from the energy-dependent analysis.

[e] The normalization of this experiment is inconsistent with both the solution and experiments at nearby energies. We have therefore floated this experiment.

[f] The normalization and individual angle errors were "folded" together by the experimentalists.

[g] The forward scattering data and the backward scattering data were measured with different experimental techniques. They have therefore been treated as independent data sets in the analysis.

[h] These are relative, unnormalized data.

[i] The normalization of these relative measurements was obtained by the experimentalists by comparison with the results of Measday (Ref. 47). We have treated these data as relative measurements.

[j] These data required a considerable renormalization and we have accordingly floated them. However, our renormalization is consistent with an energy-dependent correction factor, supplied by F. Lehar, which must be applied to the data.

where

$$B_{\pm} = B^{\pi}_{J=l\pm1}\,,$$

$$B_0 = B^{\pi}_{J\pm1,J\mp1}\,,$$

must be inserted into Eq. (1) to obtain the phase parameters $\delta_{\pm}$ and ϵ for each state with total angular momentum J. We use $(g_{NN\pi})^2 = 15$.

While this unitarization procedure differs insignificantly from our previous one for small phases, it can differ appreciably when the Born terms become large. The practical consequence of this new prescription is an easing of the strain on our energy-dependent representation. The phenomenological sum is no longer required to compensate for as large a difference in $\delta_l - \delta_l^{\mathrm{OPEC}}$ as previously when the Born terms became larger; δ_l^{OPEC} is now usually closer to δ_l.

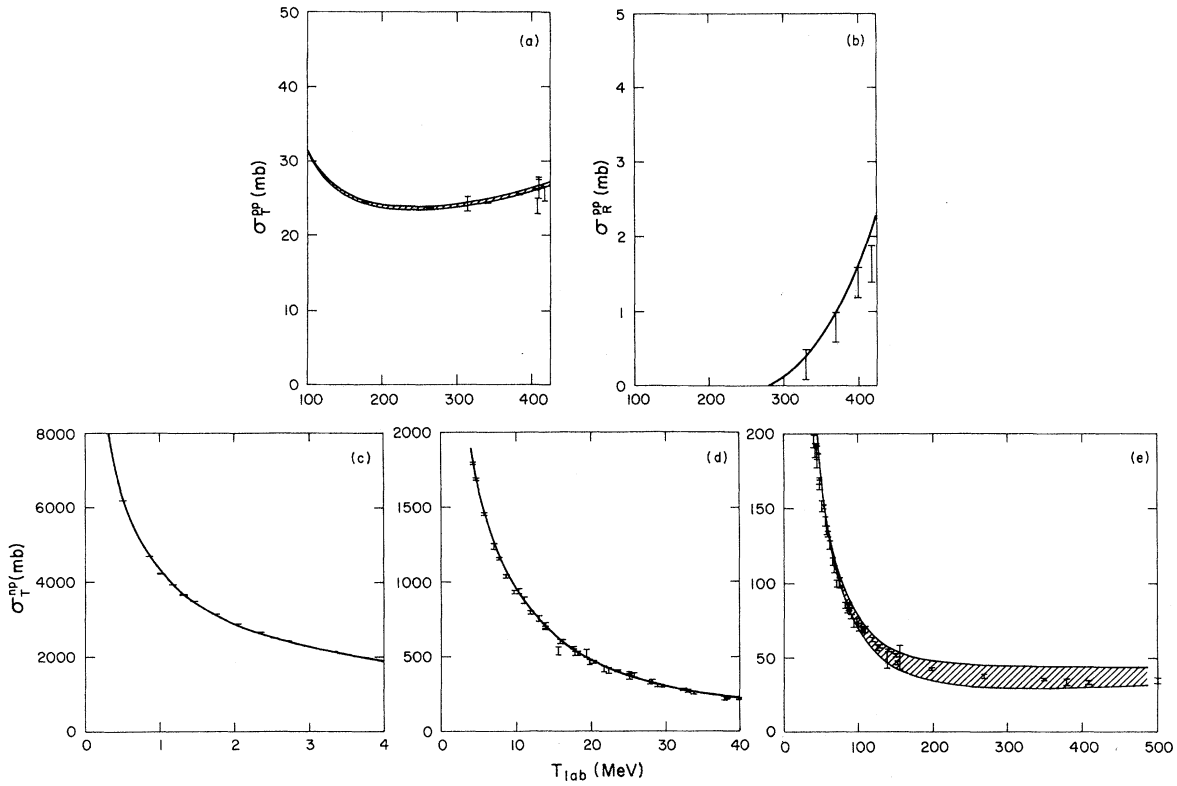

FIG. 3. A comparison of the predictions of the energy-dependent solution with experiment for (a) the p-p total cross sections, (b) the p-p reaction cross sections, (c) the n-p total cross sections from 0 to 4 MeV, (d) the n-p total cross sections from 0 to 40 MeV, and (e) the n-p total cross sections from 0 to 500 MeV.

IV. DATA BASE

The n-p data used in the present analysis are listed in Table I. Although many of the experiments have been included in previous analyses, a considerable bulk of the data, 424 data points in all, is new.

The largest additions to the data base are the 216 differential cross sections of Bersbach *et al.*[35] in the energy range 58.8 to 390.2 MeV, and the 42 differential cross sections of Bizard *et al.*[75] at 421 MeV. Other new experiments, 17 in all, are indicated in Table I by footnote b.

In general, the new data are fitted reasonably well, better in fact, in many cases, than the χ^2/datum value (which we call M) given in Table I indicates. As mentioned in previous analyses,[80] we do not feel that the phase-shift solution or the state of the data allow us to make quantitative judgments as to the accuracy or consistency of the data. We have therefore not discarded any data points, and there are data in given experiments which contribute a disproportionate amount to χ^2. As an example, consider the differential cross-section measurements of Bersbach *et al.*,[35] where M ranges from 0.36 to 2.83. At 76.7 MeV, elimination of the 49.6° datum drops M from 2.66 to 1.6; at 155.4 MeV, elimination of the 39.5° datum drops M from 2.83 to 2.01; at 168.5 MeV, elimination of the 39.6° datum drops M from 1.66 to 1.04. A new polarization experiment which stands out in this respect is that of Morris *et al.*[18] at 21.1 MeV. Elimination of the 140° datum reduces M from 3.41 to 0.38. As a point of information, we mention that if we arbitrarily discard any n-p data points whose χ^2 contribution is greater than 8, 25 data points are eliminated with a consequent decrease of 303.5 in χ^2.

There have been a number of new n-p total cross-section measurements which we have not included in our analysis,[81] not through any judgment of quality, but rather through limitations imposed by the core storage requirements of our analysis code and data base. This exclusion is of no consequence, as the difficulty experienced in the analysis of n-p scattering data is not with the number or quality of total cross sections—they are reasonably well fitted (see Fig. 3); it is with the lack of complete sets of high quality data. An illustration of the type, number, and availability of the different

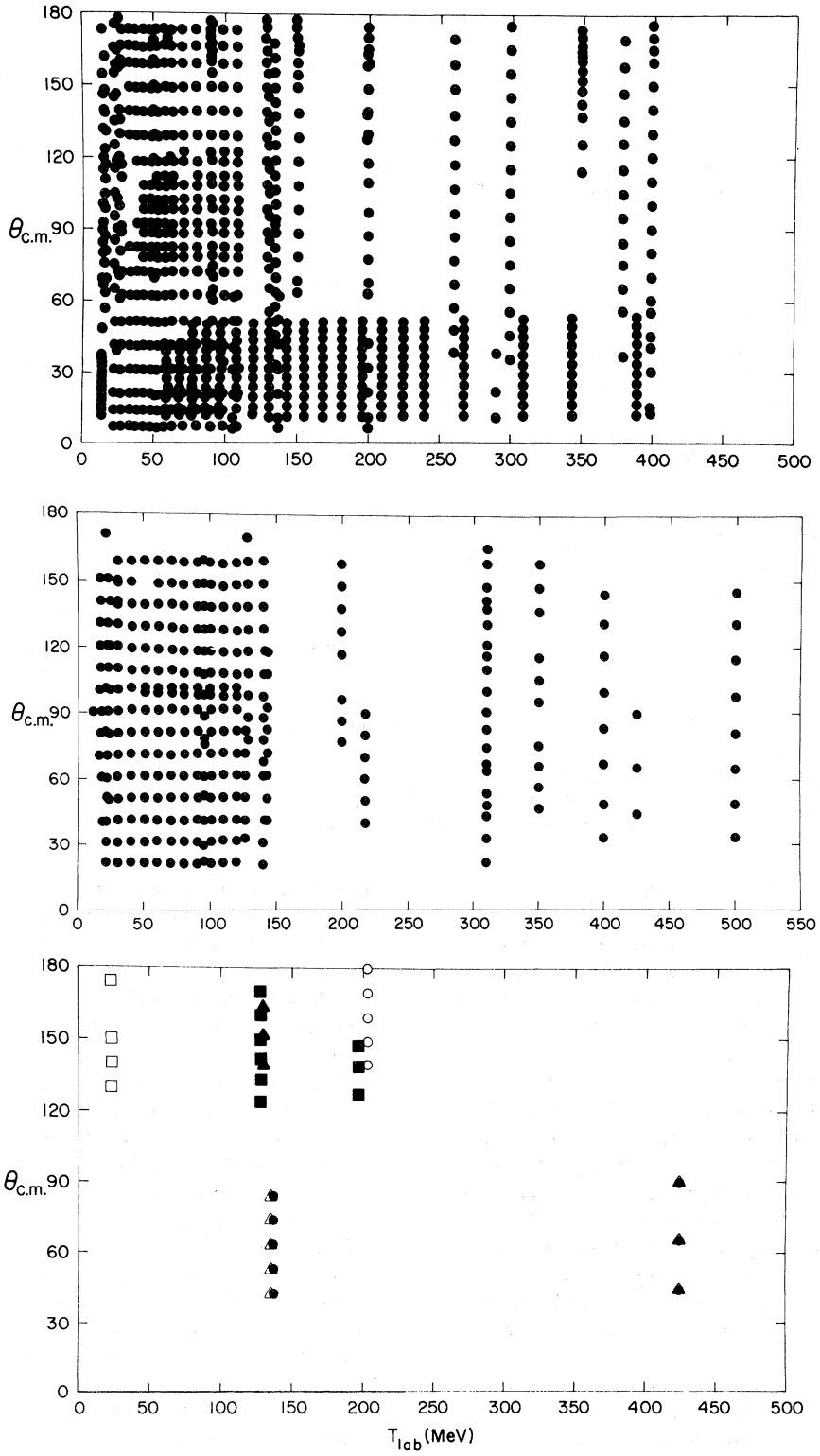

FIG. 4. The energy and angular availability of (a) differential cross sections, (b) polarization measurements, and (c) triple scattering data. In (c), ○ refers to R_T, ● refers to R, △ refers to A, ▲ refers to A_T, ■ refers to D_T, and □ refers to C_{NN}.

kinds of data is provided graphically in Fig. 4. As one can see, although cross-section and polarization measurements are readily available at most energies, triple-scattering data are virtually nonexistent over a broad energy range. It is worth noting that, although the size of the n-p data base has increased by nearly 50% since the Livermore X [$L(X)$] analysis, there has not been a single addition of triple-scattering data.

The p-p data base given in paper I is largely intact. There has been only the single addition of the 51 differential cross sections of Imai *et al.*[82]—17 data at each of the energies 4.978, 6.968, and 8.030 MeV. These data were not floated, in contrast with the low-energy procedure discussed in paper I, as we did not experience any normalization difficulties. The normalization of these experiments was quite consistent with our solution. Only the 6.968 MeV data required as much as a 0.1% renormalization. These data were fitted with an average χ^2/datum of 0.97. It was found necessary to discard the 20.03° datum at 4.978 MeV as it contributed over 11 to χ^2.

V. RESULTS

A. Energy-dependent analysis

An energy-dependent analysis was carried out simultaneously on 1284 p-p elastic scattering data in the energy range from 1 to 500 MeV and 1386 n-p elastic scattering data in the energy range from 0 to 425 MeV. A number of different analyses were run using different choices for the number of free parameters. Our final selection uses a total of 46 phenomenological parameters to represent the scattering amplitude in this range—27 for the isovector phases and 19 for the isoscalar. This choice puts the $I=0$ and $I=1$ phases on as equitable a basis as possible, considering the state of the data. The solution which was obtained for this parametrization had a χ^2 sum of 2825 for the 2670 data points (this is equivalent to an M value of 1.07). The phase shifts of this solution are depicted graphically in Figs. 1 and 2. Table I gives a complete listing of the n-p data base and the M values and normalization constants for the individual data sets which result from the analysis. A complete description of the energy-dependent parametrization is given in Secs. II and III.

The p-p phases remain essentially unchanged from their paper I values. With the exception of the ϵ_1 parameter, the n-p phases are quite similar to the Livermore X values at low energy; however, the high energy values have changed significantly in some instances. For example, the $^1P_1$ phase has changed by more than a standard deviation at 425 MeV, from −35.5° to −40°. This indicates that there is still considerable variation possible in the n-p phases in the high-energy region of the analysis. Values for the energy-dependent phase shifts are given in Tables II–IV. Values obtained for the phenomenological expansion parameters α_{ii} are given in Table V.

In conclusion, while the simultaneous search of the parameters used to represent the isovector and isoscalar phases is a novelty, we do not feel that any particular advantage was realized. The isovector phase shifts are virtually unchanged from their paper I values, the slight increase in χ^2 being due to the decreased number of phenomenological parameters used to represent the $I=1$ phases. The quality of the p-p data is so much better than the n-p data that the n-p data have only a small statistical impact in the determination of the isovector phases. Use of the representation numbers shown in Tables V and VIII reproduces all digits of all predicted values shown in Tables I, II, III, IV, and VII.

B. Single-energy analyses

Single-energy analyses were performed on the combined n-p and p-p data in energy bands centered at 25, 50, 100, 150, 200, 325, and 425 MeV. The results of these analyses are summarized in Table VI.

These analyses differ from previous analyses in two important respects. First, at each energy the "peripheral waves," that is, those which were not varied in the search, were taken from the energy-dependent analysis and not from OPEC. The remaining phase shifts were varied by adding a constant to the energy-dependent phases over the range of the energy band. This gives each phase a local energy dependence identical to the value obtained from the energy-dependent result. These modifications allowed broader energy bands to be employed, and consequently a larger number (1889) of the complete data base (2670) were incorporated in the analyses. Second, the charge splitting described in Sec. II has been employed. A large number of analyses were performed at each energy, with varying numbers of phases searched. The final choice of solutions was a compromise between having too restrictive a representation and having so many parameters that nothing definitive could be concluded from the analysis.

At the lower energies (25, 50, and 100 MeV), it was found that the $^1S_0^{np}$ phase did not search significantly away from the energy-dependent result and, moreover, that its inclusion in the search resulted in unrealistically large errors on the phase shifts. The single-energy phase shifts tabulated in Table VI, and depicted graphically in Figs. 1 and 2 are the results of single-energy analyses with the $^1S_0^{np}$

TABLE II. p-p isovector phase shifts from the combined energy-dependent solution.

T_{lab}	^1S	$^3P_0$	$^3P_1$	$^1D_2$	$*^1D_2$	$^3P_2$	E_2	$^3F_2$	$^3F_3$	$^1G_4$	$^3F_4$	E_4	$^3H_4$	$^3H_5$	$^3H_6$
1	32.49	0.13	−0.08	0.00	1.00	0.01	0.00	0.00	−0.00	0.00	0.00	0.00	0.00	−0.00	0.00
5	54.69	1.51	−0.88	0.04	1.00	0.22	−0.05	0.00	−0.01	0.00	0.00	0.00	0.00	−0.00	0.00
10	54.94	3.52	−2.01	0.17	1.00	0.66	−0.20	0.01	−0.03	0.00	0.00	0.00	0.00	−0.00	0.00
25	48.40	8.26	−4.81	0.69	1.00	2.46	−0.79	0.10	−0.23	0.04	0.03	−0.05	0.00	−0.02	0.00
50	39.16	11.85	−8.15	1.65	1.00	5.67	−1.66	0.30	−0.68	0.16	0.15	−0.19	0.03	−0.09	0.01
75	31.99	12.29	−10.81	2.58	1.00	8.49	−2.25	0.48	−1.11	0.31	0.35	−0.34	0.06	−0.02	0.02
100	25.96	11.09	−13.19	3.48	1.00	10.79	−2.61	0.63	−1.47	0.45	0.58	−0.47	0.09	−0.32	0.04
125	20.66	9.03	−15.40	4.36	1.00	12.62	−2.81	0.74	−1.77	0.60	0.84	−0.60	0.13	−0.44	0.06
150	15.89	6.52	−17.48	5.20	1.00	14.07	−2.88	0.83	−2.02	0.74	1.11	−0.72	0.15	−0.56	0.09
175	11.54	3.80	−19.47	6.01	1.00	15.18	−2.88	0.88	−2.23	0.88	1.38	−0.83	0.18	−0.67	0.12
200	7.54	1.02	−21.35	6.79	1.00	16.03	−2.80	0.92	−2.42	1.02	1.65	−0.95	0.20	−0.77	0.14
225	3.83	−1.76	−23.16	7.53	1.00	16.66	−2.68	0.94	−2.58	1.15	1.91	−1.07	0.21	−0.87	0.17
250	0.38	−4.48	−24.88	8.24	1.00	17.10	−2.52	0.95	−2.72	1.28	2.17	−1.19	0.21	−0.95	0.20
275	−2.84	−7.12	−26.52	8.92	1.00	17.40	−2.33	0.94	−2.85	1.41	2.41	−1.32	0.21	−1.03	0.23
300	−5.85	−9.65	−28.09	9.56	1.00	17.57	−2.12	0.93	−2.97	1.53	2.64	−1.45	0.21	−1.11	0.26
325	−8.69	−12.06	−29.59	10.18	0.99	17.64	−1.90	0.92	−3.08	1.66	2.87	−1.59	0.20	−1.17	0.29
350	−11.35	−14.37	−31.03	10.77	0.98	17.63	−1.67	0.90	−3.19	1.78	3.08	−1.74	0.19	−1.23	0.32
375	−13.87	−16.55	−32.41	11.34	0.97	17.54	−1.42	0.88	−3.28	1.89	3.28	−1.89	0.18	−1.29	0.35
400	−16.24	−18.63	−33.73	11.88	0.95	17.39	−1.18	0.85	−3.38	2.00	3.48	−2.05	0.16	−1.34	0.38
425	−18.49	−20.59	−35.00	12.40	0.92	17.19	−0.93	0.82	−3.46	2.11	3.66	−2.22	0.14	−1.39	0.41
450	−20.61	−22.45	−36.21	12.89	0.88	16.95	−0.68	0.80	−3.55	2.22	3.84	−2.39	0.12	−1.43	0.44
475	−22.63	−24.21	−37.38	13.36	0.84	16.68	−0.43	0.77	−3.63	2.33	4.00	−2.56	0.09	−1.47	0.47
500	−24.54	−25.87	−38.50	13.82	0.78	16.38	−0.18	0.74	−3.71	2.43	4.16	−2.74	0.06	−1.50	0.50
525	−26.36	−27.44	−39.58	14.25	0.70	16.05	0.07	0.71	−3.78	2.53	4.31	−2.92	0.04	−1.54	0.53
550	−28.09	−28.92	−40.61	14.67	0.61	15.71	0.31	0.68	−3.86	2.62	4.46	−3.11	0.01	−1.57	0.55

TABLE III. n-p isovector phase shifts from the combined energy-dependent solution.

T_{lab}	^1S	$^3P_0$	$^3P_1$	$^1D_2$	$*^1D_2$	$^3P_2$	E_2	$^3F_2$	$^3F_3$	$^1G_4$	$^3F_4$	E_4	$^3H_4$	$^3H_5$	$^3H_6$
1	62.41	0.22	−0.13	0.00	1.00	0.02	0.00	0.00	−0.00	0.00	0.00	0.00	0.00	−0.00	0.00
5	64.21	1.89	−1.10	0.05	1.00	0.28	−0.07	0.00	−0.01	0.00	0.00	0.00	0.00	−0.00	0.00
10	60.48	4.13	−2.36	0.20	1.00	0.78	−0.23	0.01	−0.04	0.00	0.00	0.00	0.00	−0.00	0.00
25	51.10	9.11	−5.32	0.77	1.00	2.73	−0.88	0.11	−0.26	0.05	0.03	−0.05	0.00	−0.02	0.00
50	40.46	12.61	−8.74	1.77	1.00	6.11	−1.79	0.32	−0.74	0.18	0.16	−0.20	0.03	−0.10	0.01
75	32.74	12.80	−11.43	2.74	1.00	9.02	−2.39	0.51	−1.18	0.33	0.37	−0.36	0.06	−0.21	0.02
100	26.56	11.33	−13.83	3.68	1.00	11.38	−2.75	0.67	−1.55	0.48	0.62	−0.50	0.10	−0.34	0.04
125	21.37	9.02	−16.06	4.58	1.00	13.25	−2.94	0.78	−1.85	0.63	0.89	−0.63	0.13	−0.46	0.07
150	16.88	6.29	−18.17	5.44	1.00	14.71	−3.01	0.86	−2.11	0.78	1.17	−0.75	0.16	−0.58	0.09
175	12.91	3.37	−20.16	6.27	1.00	15.83	−2.99	0.92	−2.33	0.92	1.45	−0.87	0.19	−0.70	0.12
200	9.36	0.40	−22.07	7.07	1.00	16.68	−2.91	0.95	−2.52	1.06	1.72	−0.99	0.20	−0.80	0.15
225	6.15	−2.53	−23.88	7.83	1.00	17.30	−2.78	0.97	−2.68	1.20	1.99	−1.11	0.22	−0.90	0.18
250	3.24	−5.40	−25.62	8.55	1.00	17.74	−2.60	0.98	−2.83	1.33	2.25	−1.24	0.22	−0.99	0.21
275	0.56	−8.16	−27.27	9.24	1.00	18.02	−2.41	0.97	−2.96	1.46	2.50	−1.37	0.22	−1.07	0.24
300	−1.90	−10.80	−28.86	9.90	1.00	18.18	−2.19	0.96	−3.08	1.59	2.74	−1.50	0.22	−1.15	0.27
325	−4.18	−13.32	−30.37	10.54	0.99	18.23	−1.95	0.94	−3.19	1.71	2.97	−1.65	0.21	−1.21	0.30
350	−6.29	−15.71	−31.82	11.14	0.98	18.20	−1.71	0.92	−3.29	1.84	3.19	−1.80	0.20	−1.28	0.34
375	−8.26	−17.98	−33.21	11.71	0.97	18.09	−1.46	0.90	−3.39	1.95	3.39	−1.96	0.18	−1.33	0.37
400	−10.10	−20.13	−34.54	12.27	0.95	17.93	−1.20	0.87	−3.48	2.07	3.59	−2.12	0.16	−1.38	0.40
425	−11.82	−22.16	−35.81	12.79	0.92	17.71	−0.94	0.84	−3.57	2.18	3.78	−2.29	0.14	−1.43	0.43
450	−13.43	−24.08	−37.04	13.30	0.88	17.46	−0.68	0.81	−3.66	2.29	3.96	−2.46	0.12	−1.47	0.46
475	−14.95	−25.90	−38.21	13.78	0.84	17.17	−0.43	0.78	−3.74	2.40	4.13	−2.64	0.09	−1.51	0.48
500	−16.38	−27.61	−39.34	14.24	0.78	16.85	−0.17	0.75	−3.82	2.50	4.29	−2.82	0.07	−1.55	0.51

TABLE IV. n-p isoscalar phase shifts from the combined energy-dependent solution.

T_{lab}	$^1P_1$	$^3S_1$	E_1	$^3D_1$	$^3D_2$	$^1F_3$	$^3D_3$	E_3	$^3G_3$	$^3G_4$	$^1H_5$	$^3G_5$	E_5
1	−0.18	147.81	0.06	−0.00	0.01	−0.00	0.00	−0.00	−0.00	0.00	−0.00	−0.00	−0.00
5	−1.34	118.31	0.28	−0.15	0.26	−0.01	0.01	0.02	−0.00	0.00	−0.00	−0.00	−0.00
10	−2.56	102.83	0.29	−0.57	0.98	−0.08	0.03	0.10	−0.00	0.02	−0.00	−0.00	−0.00
25	−4.58	81.05	−0.24	−2.58	4.10	−0.49	0.18	0.63	−0.07	0.20	−0.04	−0.01	0.05
50	−6.64	63.02	−0.81	−6.25	9.47	−1.26	0.67	1.76	−0.30	0.82	−0.19	−0.06	0.24
75	−8.95	51.14	−0.52	−9.39	13.94	−1.87	1.27	2.78	−0.61	1.57	−0.39	−0.12	0.52
100	−11.59	41.82	0.38	−11.94	17.44	−2.31	1.88	3.61	−0.94	2.33	−0.60	−0.19	0.82
125	−14.41	34.03	1.66	−14.00	20.12	−2.61	2.44	4.27	−1.28	3.07	−0.78	−0.24	1.11
150	−17.27	27.35	3.13	−15.65	22.11	−2.81	2.91	4.80	−1.62	3.76	−0.95	−0.29	1.40
175	−20.09	21.56	4.65	−16.96	23.55	−2.93	3.31	5.23	−1.94	4.42	−1.09	−0.32	1.66
200	−22.82	16.49	6.15	−17.97	24.53	−2.99	3.63	5.58	−2.24	5.03	−1.21	−0.34	1.91
225	−25.42	12.04	7.59	−18.73	25.16	−3.01	3.88	5.85	−2.53	5.60	−1.31	−0.35	2.14
250	−27.89	8.10	8.93	−19.27	25.48	−3.00	4.06	6.07	−2.80	6.13	−1.40	−0.35	2.35
275	−30.22	4.60	10.17	−19.61	25.56	−2.96	4.19	6.25	−3.07	6.63	−1.47	−0.34	2.55
300	−32.42	1.47	11.30	−19.79	25.43	−2.90	4.26	6.39	−3.31	7.10	−1.52	−0.33	2.73
325	−34.48	−1.35	12.34	−19.83	25.15	−2.83	4.29	6.50	−3.55	7.55	−1.56	−0.31	2.90
350	−36.41	−3.90	13.29	−19.74	24.72	−2.74	4.28	6.59	−3.77	7.97	−1.60	−0.29	3.05
375	−38.22	−6.23	14.15	−19.55	24.19	−2.64	4.24	6.66	−3.98	8.36	−1.62	−0.26	3.19
400	−39.92	−8.37	14.94	−19.28	23.56	−2.54	4.16	6.71	−4.19	8.74	−1.63	−0.23	3.33
425	−41.51	−10.35	15.65	−18.93	22.86	−2.43	4.06	6.74	−4.38	9.09	−1.64	−0.19	3.45
450	−43.00	−12.19	16.30	−18.51	22.09	−2.31	3.94	6.76	−4.56	9.43	−1.64	−0.15	3.56
475	−44.40	−13.90	16.89	−18.04	21.28	−2.20	3.79	6.78	−4.74	9.75	−1.63	−0.12	3.67
500	−45.71	−15.52	17.42	−17.53	20.43	−2.08	3.63	6.78	−4.91	10.06	−1.62	−0.08	3.77

TABLE V. Values obtained for the phenomenological expansion parameters α_{l1} in the energy-dependent analysis.

Partial wave	α_{l1}	α_{l2}	α_{l3}
$^1S_0$	77.1	−176.4	
$^3P_0$	225.5	−892.6	605.2
$^3P_1$	69.0	−117.0	
$^1D_2$	583.3	33.9	
$^3P_2$	−121.5	741.7	−761.3
ϵ_2	−27.9	85.6	
$^3F_2$	−22.7	8.7	
$^3F_3$	39.9	−52.6	
$^1G_4$	18.1		
$^3F_4$	43.6	−62.1	
ϵ_4	131.1	−325.8	
$^3H_9$	−28.1	17.8	
$^3H_6$	16.4		
$^1S_0$ (np)	28.5	−85.2	
$^1P_1$	489.5	−1823	1383
$^3S_1$	12.8	−22.7	
ϵ_1	9.7	−19.6	
$^3D_1$	19.7	−44.0	
$^3D_2$	266.0	−582.5	
$^1F_3$	15.4		
$^3D_3$	125.2	−193.5	
ϵ_3	−28.4		
$^3G_3$	6.6		
$^3G_4$	−9.4		

phase fixed at the energy-dependent values.

In any energy-dependent analysis, the question of an overly restrictive parametrization is a problem which must be explored. One measure of validity of the energy-dependent solution is a comparison of the χ^2 obtained in the single-energy analysis on a given data set with the χ^2 resulting from that data set with the energy-dependent solution. We do this in Table VII. It is our opinion that the small differences strongly support the credibility of the energy-dependent solution.

A second question in this context is the validity of the errors on the energy-independent phase shifts, for example, in a comparison of the energy-dependent and energy-independent results. The errors on the phase shifts given in Tables II–IV are derived from the diagonal elements of the corresponding error matrix, which assumes that χ^2 is quadratic about the solution value. Strictly speaking, this assumption is always at least locally correct. The question is whether the energy-dependent results lie within its domain of validity. Consider that the inverse error matrix, defined by

$$A_{mn} = \frac{\partial^2}{\partial P_m \partial P_n} \chi^2 ,$$

where the P_m are the parameters varied in the search, and which depends explicitly on the quadratic assumption, can be used to represent the

TABLE VI. Single-energy phase shifts.

Energy (MeV)	25	50	100	150	200	325	425
				Isovector			
$^1S_0$	47.94±0.37	39.09±0.27	24.98±0.46	14.89±0.49	6.55±0.46	−11.03±1.11	−18.72±1.08
$^1D_2$	0.78±0.03	1.67±0.06	3.86±0.13	5.44±0.08	7.08±0.13	10.28±0.28	12.27±0.49
$^3P_0$	9.51±0.22	12.48±0.34	12.04±1.42	5.66±0.43	0.06±0.48	−14.37±1.41	−17.59±1.10
$^3P_1$	−5.42±0.12	−8.75±0.15	−14.04±0.26	−18.11±0.14	−21.81±0.28	−29.44±0.75	−34.67±0.87
$^3P_2$	2.63±0.05	6.11±0.08	11.03±0.18	14.78±0.09	16.26±0.19	18.01±0.43	20.15±0.72
ϵ_2	−0.86±0.50	−1.69±0.08	−2.86±0.12	−2.98±0.06	−2.98±0.13	−2.09±0.34	−0.84±0.47
$^3F_2$			0.69±0.50	1.07±0.18	1.12±0.26	1.70±0.47	2.13±0.44
$^3F_3$			−1.55±0.50	−2.23±0.14	−2.64±0.18	−4.15±0.55	−2.66±0.43
$^3F_4$			0.60±0.50	1.23±0.09	1.89±0.15	3.07±0.20	4.09±0.32
				Isoscalar			
$^1S_0$	(51.22)	(40.69)	(26.91)	(17.24)	(9.69)	(−4.00)	(−11.80)
$^1P_1$	−4.49±0.94	−4.33±0.74	−12.62±1.13	−19.83±1.10	−22.16±1.55	−36.19±1.14	−39.73±1.55
$^1F_3$		−1.24±0.50	−2.28±0.50	−2.02±0.36	−3.70±0.62	−2.48±0.59	−2.60±0.63
$^3S_1$	79.89±0.88	61.35±0.57	42.43±0.59	27.04±0.55	16.81±1.11	−2.03±2.43	−7.89±2.10
ϵ_1	0.71±0.84	0.10±1.30	0.07±0.96	4.30±0.63	5.99±0.68	17.68±1.89	14.48±1.39
$^3D_1$	−2.83±0.42	−6.71±0.24	−12.18±0.38	−14.95±0.42	−17.64±1.07	−21.48±1.58	−17.73±1.17
$^3D_2$	4.29±0.77	10.56±0.37	16.18±0.74	22.46±0.50	25.45±0.76	19.88±1.49	22.93±1.17
$^3D_3$		0.68±0.50	1.93±0.50	2.74±0.36	3.63±0.61	3.36±0.85	4.86±0.82
ϵ_3		1.74±0.50	3.61±0.50	4.43±0.23	6.29±0.33	6.51±0.69	6.12±0.54

data at each energy. Then, one measure of validity of the quadratic assumption is a comparison of the χ^2 value obtained from this representation for the phase shifts as predicted by the energy-dependent solution with the χ^2 value from the energy-dependent solution, which is obtained directly from the data. As can be seen in Table VII, only a small discrepancy exists, which systematically grows larger with energy. A more detailed study of the χ^2 hypersurface at 50 and 325 MeV reveals

TABLE VII. Summary of energy-independent solutions.

Lab kinetic energy (MeV)	Data type	Energy band (MeV)	Number of data	Number of phases searched	χ^2 Energy-dep. solution	χ^2 Energy-ind. solution	χ^2 (total) Error matrix
25	*p-p*	19.2–30	45	5	27	21	126
	n-p	19.6–30	144	5	98	84	
50	*p-p*	41.1–60	101	6	101	94	298
	n-p	40–60.9	188	5	194	177	
100	*p-p*	86–107	112	6	92	85	375
	n-p	86.5–110	211	5	282	271	
150	*p-p*	127–174	220	9	198	185	459
	n-p	126–170	208	8	262	247	
200	*p-p*	210–213	64	9	59	51	162
	n-p	181–217	89	8	104	81	
325	*p-p*	305–345	159	9	145	137	260
	n-p	300–350	92	8	123	81	
425	*p-p*	394–460	161	9	156	141	353
	n-p	390–425	95	8	186	162	
Totals	*p-p*		862		778	714	2033
	n-p		1027		1249	1103	

an irregular structure which will be dealt with more extensively in future papers.

In conclusion, as a best estimate of the phase shifts, we recommend taking the energy-dependent values and the energy-independent errors.

APPENDIX A

In this appendix, we describe our parametrization of the $I=0$, $J=1$ partial-wave amplitudes. The method we choose is similar to that of Wong,[78] except that we use a K-matrix formalism rather than an effective-range expansion of the T matrix. The relationship between the K matrix and T matrix,

$$T = K(1 - iK)^{-1},$$

may be used to relate the K matrix elements to the usual nuclear-bar phase shifts, i.e.,

$$\begin{aligned} T_S &= e^{i\delta_S}\sin\delta_S + i\sin^2 e^{2i\delta_S} = (K_S - id)/D\,, \\ T_0 &= \sin\epsilon\cos\epsilon\, e^{i(\delta_S+\delta_D)} = K_0/D\,, \\ T_L &= e^{i\delta_D}\sin\delta_D + i\sin^2\epsilon\, e^{2i\delta_D} = (K_D - id)/D\,, \end{aligned} \tag{A1}$$

where

$$\begin{aligned} d &\equiv K_S K_D - K_0^2\,, \\ D &\equiv 1 - d - i(K_S + K_D)\,. \end{aligned}$$

In these expressions, the S and D subscripts refer to the $l=0$ and $l=2$ components, respectively, and the "0" subscript refers to the off-diagonal element of T and K.

It is of particular interest to examine the above equations in the low-energy limit. The phase parameters δ_S, ϵ, and δ_D behave at threshold like p, p^3, and p^5, respectively, where p is the center-of-mass momentum, so that at threshold to order p^5 we obtain

$$\begin{aligned} T_S &\simeq e^{i\delta_S}\sin\delta_S \simeq K_S/D\,, \\ T_0 &\simeq \sin\epsilon\cos\epsilon\, e^{i\delta_S} \simeq K_0/D\,, \\ T_D &\simeq e^{i\delta_D}\sin\delta_D \simeq K_D/(1 - iK_D)\,, \\ D &\simeq 1 - iK_S\,. \end{aligned} \tag{A2}$$

Thus at threshold to order p^5 we find

$$\begin{aligned} &K_S \simeq \tan\delta_S\,, \\ &\sin\epsilon\cos\epsilon \simeq K_0\cos\delta_S\,. \end{aligned} \tag{A3}$$

Since the S-wave phase shift δ_S is normalized to π at threshold and goes through $\frac{1}{2}\pi$ at about 18 MeV, these equations imply that K_0 is opposite in sign to ϵ below 18 MeV and that ϵ must change sign at the same energy δ_S does if K_0 does not.

The deuteron constraints require that $D=0$ when the center-of-mass energy E is equal to the deuteron binding energy $-E_d$ ($E_d = 4.449$ MeV), and that

$$\begin{aligned} &\left(\frac{M}{2}\right)^{1/2}\frac{(E+E_d)}{\hbar c}\,T_s\Big|_{E=-E_d} = \Gamma = \frac{-1}{\hbar c}\left(\frac{M}{2E_d}\right)^{1/2}\frac{1}{D'}\Big|_{E=-E_d}, \\ &K_s|_{E=-E_d} = -i\,, \\ &K_0|_{E=-E_d} = i\rho\,, \end{aligned} \tag{A4}$$

where Γ and ρ are defined in a manner similar to that of Wong.[78] Following Wong, we interpret Eqs. (A2) in the sense of a dispersion relation for K_0

$$K_0^\pi = \frac{1}{\pi}\int_{-m_\pi^2/2M}^{-\infty} \mathrm{Im}T_0^\pi\,\frac{(1 - iK_s)}{(E' - E)}\,dE'\,, \tag{A5}$$

where the left-hand discontinuity in T_0 is taken from pion exchange (the superscript π is used to denote this fact). In this expression, m_π is the pion mass and M is the nucleon mass.

Using this expression, we parametrize the K matrix elements according to

$$\begin{aligned} K_S &= \frac{E^{1/2}}{E_A}\,\frac{(E_A+E_B)(E_C-E)}{(E-E_B)(E_C+E_A)} + A^S f_{11}\,, \\ K_0 &= K_0^\pi + \sum_{n=1}^{2} A_n^0 f_{1n}\,, \\ K_D &= B_D^\pi + \sum_{n=1}^{2} A_n^D f_{2n}\,, \end{aligned} \tag{A6}$$

where the f_{in} are the basis functions described in the main body of the paper and B_D is the OPEC term for the $^3D_1$ state. The quantities E_A, E_B, E_C, A^S, A_1^0, A_2^0, A_1^D, and A_2^D are adjustable parameters.

The motivation for this particular choice of parametrization is twofold. First, the use of the basis functions f_{in} and the functions K_0^π and B_D^π insure that the matrix elements will have at least approximately the appropriate discontinuity across the near end of the left-hand cut. Second, the additional energy dependence in K_S represents the uncoupled S-wave phase quite well below 400 MeV if we choose $E_A = -E_d$ (where D must have a zero), $E_B \simeq 18$ MeV (where δ_S falls through $\frac{1}{2}\pi$), and

TABLE VIII. Values obtained for the phenomenological parameters in Eq. (A6).

Parameter	Value
E_A	4.41 MeV
E_B	17.13 MeV
E_C	515.8 MeV
A^S	−11.53
A_1^0	−44.99
A_2^0	1.32
A_1^D	−188.2
A_2^D	444.2

$E_C \simeq 300$ MeV (where δ_S has a zero). For the energy-dependent analysis E_A was adjusted such as to produce a zero in D at the deuteron binding energy and the remaining seven parameters were adjusted to fit the low energy (below 50 MeV) cross sections and the phase parameters δ_S, E, and δ_D between 0 and 450 MeV.

The resultant representation gives a precise fit to the low-energy cross sections and a reasonable fit to the phase parameters below 500 MeV. The values obtained for the adjustable parameters in Eq. (A6) are given in Table VIII. The deuteron parameters which resulted were $\Gamma = (-0.766 \pm 0.002)$ fm^{-1} and $\rho = 0.022 \pm 0.008$. The S-wave scattering length and effective range obtained were

$$a = (1.737 \pm 0.006) \text{ fm},$$

$$r = (5.380 \pm 0.005) \text{ fm}.$$

These latter values are consistent with the values given in Table 2 of Signell.[79] The phases obtained are depicted as solid lines in the $^3S_1$, ϵ_1, and $^3D_1$ graphs in Fig. 1. Notice that the sign of ϵ_1 changes at $E \simeq 20$ MeV. This fact is undoubtedly important to the analysis of the 50 MeV data which has persistently demanded a negative ϵ_1.

---

*Supported by a grant from the U.S. Energy Research and Development Administration.

[1]C. E. Engelke, R. E. Benenson, E. Melkonian, and J. M. Lebowitz, Phys. Rev. 129, 324 (1963).
[2]P. J. Clements and A. Langsford, Phys. Lett. 30B, 25 (1969); P. J. Clements (private communication).
[3]R. E. Fields, R. L. Becker, and R. K. Adair, Phys. Rev. 94, 389 (1954).
[4]C. L. Storrs and D. H. Frisch, Phys. Rev. 95, 1252 (1954).
[5]E. M. Hafner, W. F. Hornyak, C. E. Falk, G. Snow, and T. Coor, Phys. Rev. 89, 204 (1952).
[6]A. Bratenahl, J. M. Peterson, and J. P. Stoering, Phys. Rev. 110, 927, (1958).
[7]G. S. Mutchler and J. E. Simmons, Phys. Rev. C 4, 67 (1971).
[8]J. Arvienx and J. Pouxe, Phys. Lett. 32B, 468 (1970).
[9]J. C. Allred, A. H. Armstrong, and L. D. Rosen, Phys. Rev. 91, 90 (1953).
[10]A. Suhami and R. Fox, Phys. Lett. 24, 173 (1967).
[11]J. D. Seagrave, Phys. Rev. 97, 757 (1955).
[12]H. L. Poss, E. O. Salant, G. A. Snow, and L. C. L. Yuan, Phys. Rev. 87, 11 (1952).
[13]W. T. Morton, Proc. Phys. Soc. (London) 91, 899 (1967).
[14]P. H. Bowen, J. P. Scanlon, G. H. Stafford, J. J. Thresher, and P. E. Hodgson, Nucl. Phys. 22, 640 (1961).
[15]R. Garret, A. Chisolm, D. Brown, J. C. Puder, and H. N. Bürgisser, Nucl. Phys. A196, 421 (1972).
[16]W. Benson, R. L. Walter, and T. H. May, Phys. Rev. Lett. 8, 66 (1962).
[17]D. T. L. Jones, and F. D. Brooks, Nucl. Phys. A222, 79 (1974); D. T. L. Jones (private communication).
[18]C. L. Morris, T. K. O'Malley, J. W. May, Jr., and S. T. Thornton, Phys. Rev. C 9, 924 (1974).
[19]J. M. Peterson, A. Bratenahl, and J. P. Stoering, Phys. Rev. 120, 521 (1960).
[20]D. E. Groce and B. D. Sowerby, Nucl. Phys. 83, 199 (1966).
[21]R. B. Day, R. L. Mills, J. E. Perry, Jr., and F. Scherb, Phys. Rev. 98, 279 (1955).
[22]A. Langsford, P. H. Bowen, G. C. Cox, G. B. Huxtable, and R. A. J. Riddle, Nucl. Phys. 74, 241 (1965).
[23]E. R. Flynn and P. J. Bendt, Phys. Rev. 128, 1268 (1962).
[24]J. P. Scanlon, G. H. Stafford, J. J. Thresher, P. H. Bowen, and A. Langsford, Nucl. Phys. 41, 401 (1963).
[25]J. J. Malanify, J. P. Bendt, T. R. Roberts, and J. E. Simmons, Phys. Rev. Lett. 17, 481 (1966), and private communication; J. E. Simmons, Rev. Mod. Phys. 39, 542 (1967).
[26]R. B. Perkins and J. E. Simmons, Phys. Rev. 130, 272 (1963).
[27]L. N. Rothenberg and T. G. Masterson, Bull. Am. Phys. Soc. 14, 511 (1969); L. N. Rothenberg (private communication). These dates were later published by L. N. Rothenberg, Phys. Rev. C 1, 1226 (1969).
[28]T. W. Burrows, Phys. Rev. C 7, 1306 (1973).
[29]T. G. Masterson, Phys. Rev. C 6, 690 (1972).
[30]F. P. Brady, W. J. Knox, J. A. Jungerman, M. R. McGie, and R. L. Walraven, Phys. Rev. Lett. 25, 1628 (1970).
[31]Michael McNaughton (private communication).
[32]R. A. Eldred, Ph.D. thesis, U. of California, (unpublished); and private communication.
[33]A. E. Taylor and E. Wood, Phil. Mag. 44, 95 (1952).
[34]T. C. Montgomery (private communication from M. McNaughton).
[35]A. J. Bersbach, R. E. Mishke, and T. J. Perlin (private communication from R. E. Mishke).
[36]M. J. Saltmarsh, C. R. Bingham, M. L. Halbert, C. A. Lindemann, and A. van der Wonde, Oak Ridge National Laboratory (unpublished). These data are listed in a preliminary form in a phase-shift analysis of R. A. Arndt, J. Binstock, and R. Bryan, Texas A&M report, 1972 (unpublished).
[37]P. Hillman, R. H. Stahl, and N. F. Ramsey, Phys. Rev. 96, 115 (1954).
[38]D. F. Measday and J. N. Palmieri, Nucl. Phys. 85, 142 (1966).
[39]R. G. Stahl and N. F. Ramsey, Phys. Rev. 96, 1310 (1954).
[40]G. H. Stafford, C. Whitehead, and P. Hillman, Nuovo Cimento 5, 1589 (1957).
[41]J. J. Tresher, R. G. P. Voss, and R. Wilson, Proc. Roy. Soc. (London) A229, 492 (1955).
[42]A. S. Carroll, P. M. Patel, N. Strax, and D. Miller, Phys. Rev. 134, B595 (1964).
[43]R. K. Hobbie and D. Miller, Phys. Rev. 120, 2201 (1960).
[44]P. M. Patel, A. Carroll, N. Strax, and D. Miller, Phys. Rev. Lett. 8, 491 (1962).
[45]W. G. Collins, Jr., and D. G. Miller, Phys. Rev. 134,

B575 (1964).
[46]N. Strax (unpublished); R. Wilson (private communication).
[47]D. F. Measday, Phys. Rev. 142, 584 (1966).
[48]T. C. Randle, D. M. Skyrme, M. Snowden, A. E. Taylor, F. Uridge, and E. Wood, Proc. Phys. Soc. (London) A69, 760 (1956).
[49]R. A. Hoffman, J. Lefrancois, E. H. Thorndyke, and R. Wilson, Phys. Rev. 125, 973 (1962); J. Lefrancois, R. A. Hoffman, E. H. Thorndyke, and R. Wilson, *ibid.* 131, 1660 (1963); A. H. Cromer and E. H. Thorndyke, *ibid.* 131, 1680 (1963).
[50]J. A. Edington, V. J. Howard, S. S. Das Gupta, I. M. Blair, B. E. Bonner, F. P. Brady, M. W. McNaughton, and N. M. Stewart, Rutherford Report No. RL-73-073, July, 1973 (unpublished).
[51]G. R. Mott, G. L. Guernsey, and B. K. Nelson, Phys. Rev. 88, 9 (1952).
[52]G. H. Stafford and C. Whitehead, Proc. Phys. Soc. (London) 79, 430 (1962).
[53]A. F. Kuckes and R. Wilson, Phys. Rev. 121, 1226 (1961); A. H. Cromer and E. H. Thorndyke, *ibid.* 131, 1680 (1963).
[54]J. N. Palmieri and Janet P. Wolfe, Phys. Rev. C 3, 145 (1971).
[55]D. Spalding, A. R. Thomas, and E. H. Thorndyke, Phys. Rev. 158, 1388 (1967).
[56]A. R. Thomas, D. Spalding, and E. H. Thorndyke, Phys. Rev. 167, 1240 (1968); E. H. Thorndyke, Rev. Mod. Phys. 39, 513 (1967).
[57]Yu. M. Kazarinov and Yu. N. Simonov, Zh. Eksp. Teor. Fiz. 43, 35 (1962) [Soviet Phys.–JETP 16, 24 (1963)].
[58]N. W. Reay, E. H. Thorndyke, D. Spalding, and A. R. Thomas, Phys. Rev. 150, 801 (1966); E. H. Thorndyke, Rev. Mod. Phys. 39, 513 (1967).
[59]R. E. Warner and J. H. Tinlot, Phys. Rev. 125, 1028 (1962); E. H. Thorndyke, Rev. Mod. Phys. 39, 513 (1967).
[60]J. H. Tinlot and R. E. Warner, Phys. Rev. 124, 890 (1961); E. H. Thorndyke, Rev. Mod. Phys. 39, 513 (1967).
[61]E. Kelley, C. Leith, E. Segrè, and C. Weigand, Phys. Rev. 79, 96 (1950).
[62]J. DeJuren, Phys. Rev. 80, 23 (1950).
[63]J. W. Easley, University of California Radiation Laboratory Report No. UCRL-2693, 1954 (unpublished).
[64]J. DePanger, Phys. Rev. 99, 1447 (1955).
[65]O. Chamberlain, E. Segrè, R. D. Tripp, C. Weigand, and T. Ypsilantis, Phys. Rev. 105, 288 (1957).
[66]D. Cheng, B. MacDonald, J. A. Helland, and P. M. Ogden, Phys. Rev. 163, 1470 (1967).
[67]A. Ashmore, R. G. Jarvis, D. S. Mather, and S. K. Sen, Proc. Phys. Soc. (London) A70, 745 (1957).
[68]A. Ashmore, W. H. Range, R. T. Taylor, B. M. Townes, L. Castillejo, and R. F. Peierls, Nucl. Phys. 36, 258 (1962).
[69]R. T. Siegel, A. J. Hartzler, and W. A. Love, Phys. Rev. 101, 838 (1956).
[70]V. P. Dzhelepov, V. I. Satarov, and B. M. Golovin, Dokl. Akad. Nauk SSSR 104, 717 (1955).
[71]V. P. Dzhelepov and Yu. M. Kazarinov, Dokl. Akad. Nauk SSSR 99, 939 (1954).
[72]A. J. Hartzler, R. T. Siegel, and W. Optiz, Phys. Rev. 95, 185, 591 (1954).
[73]V. Alexander Nedzel, Phys. Rev. 94, 174 (1954).
[74]S. C. Wright, D. Shawhan, L. Pondrom, S. Olsen, and R. Haudler, Phys. Rev. 175, 1704 (1968).
[75]G. Bizard, F. Bonthonneau, J. L. Laville, F. Lefebvres, J. C. Malherbe, R. Regimbart, J. Duflo, and F. Plouin, Université de Caen report (unpublished).
[76]M. H. McGregor, R. A. Arndt, and R. M. Wright, Phys. Rev. 182, 1714 (1969). The energy-dependent phenomenological expansion bases used in this paper and in previous analyses are defined in M. H. McGregor, R. A. Arndt, and R. M. Wright, Phys. Rev. 169, 1128 (1968), formula (17), where $f_{li} \equiv F_{li}$.
[77]R. A. Arndt, R. H. Hackman, and L. D. Roper, Phys. Rev. C 9, 555 (1974).
[78]D. Y. Wong, Phys. Rev. Lett. 2, 406 (1959).
[79]P. Signell, Phys. Rev. C 2, 1171 (1970).
[80]See M. H. McGregor, R. A. Arndt, and R. M. Wright, Phys. Rev. 173, 1272 (1968).
[81]There were a large number of these cross-section measurements made in the low-energy region in a search for the structure which at one time was reported by G. Hrehuss and T. Czibók, Phys. Lett. 28B, 585 (1969). See S. Cierjacks, P. Forti, G. J. Kirouac, D. Kopsch, L. Kropp, and J. Nebe, Phys. Rev. Lett. 23, 866 (1969); R. B. Schwartz, R. A. Schrack, and H. T. Heaton, Phys. Lett. 30B, 36 (1969); T. L. Houk, Phys. Rev. C 3, 1886 (1970); P. J. Clements and A. Langsford, Phys. Lett. 30B, 25 (1969). Most of these data seem to be consistent with previous determinations of scattering lengths and effective ranges.
[82]K. Imai, K. Nisimura, N. Tamura, and H. Sato, Kyoto University Report No. KUNS 310 (unpublished); and K. Nisimura (private communication).